components involved, one at a time. One case is particularly simple, namely, if two components are added in relative amounts corresponding to the relative amounts required in two separate experiments on the pure components. In this case, the combined addition quenches at a phase that is precisely the average value of the phases for the quenchings with the two separate components. (There is a slight ambiguity in the definition of average values of phases because these are defined modulo 360°. This point will be clarified in a forthcoming paper[3] where the calculation of quenchings of general combinations will be presented.)

The consistency check has been applied to combinations of Ce^{4+} and Br^-. These components were mixed in the proportion that is predicted to quench at the average phase and added from one buret. The results agrees with the prediction, and this can be taken as a sign that the oscillations are sufficiently harmonic and that the stable and unstable manifolds are sufficiently well approximated by their tangent spaces in the region of operation of the experiments.

Dilution can be considered as removal of each species present in direct proportion to its (instantaneous) concentration. The consistency check can therefore be used to compare the result of a dilution with those of all the addition experiments. The conclusion from such a comparison is that the quenching phase of the dilution cannot be explained by the presence of any combination of concentrations of the species listed in Table I alone. Dilution of any such mixture should quench at an angle in the interval $-90° \leq \phi \leq 90°$ (having a positive cosine), a conclusion in conflict with the quenching angle of 106° (with negative cosine) actually observed. This means that one or more species that quench by addition at angles in the interval $-90° \leq \phi \leq +90°$ must be present in sufficient average concentration. This conclusion presupposes error bounds of approximately ±5° for the quenching angles (and also that there is no systematic error due to impurity, for example). The theoretical basis for the argument just given will be presented in the forthcoming paper mentioned.[3]

There are two obvious ways of using quenching experiments to obtain insight in a chemical reaction system. The most striking one is the direct reconstruction of amplitudes and phases we have presented here. It rests on the assumption that at most three independent species oscillate with appreciable amplitude but can be extended to higher dimensions.

Another way of using quenching experiments that avoids any uncertainty surrounding reconstructions is as a test of models of a reaction. Qualitative aspects of the experiments may usefully be considered.[9] It is significant, for example, that it was impossible to quench the oscillations with any of the organic chemicals tested. This fact can be taken as a direct experimental confirmation of the view embodied in most models of the BZ reaction that it is the bromine chemistry in association with Ce^{3+}/Ce^{4+} that is directly responsible for the oscillations, with the organic chemicals playing a role of sustaining the oscillations.

However, it is in *quantitative* comparisons with models that quenching experiments are potentially most useful in general. A model can be tested against experiments in several other ways, for example, by its prediction of bifurcation pattern, character and properties of oscillations, etc. But, these features typically have a complicated relation to the kinetics of a reaction system. In contrast, quenching data are directly related to the Jacobi matrix of the kinetic equations as eq 9 and 10a–c certainly show. Comparison of quenching data predicted by a model with corresponding experimental data therefore constitutes a significant quantitative test of the kinetics of the model as far as small oscillations are concerned. We shall use this approach in forthcoming papers.

Acknowledgment. We are indebted to Professor H. Försterling for supplying the sample of $HBrO_2$. We thank Merete Torpe for her valuable technical assistance.

Registry No. Ce^{4+}, 16065-90-0; $HBrO_2$, 37691-27-3; Br^-, 24959-67-9; HBrO, 13517-11-8; Br_2, 7726-95-6; bromomalonic acid, 600-31-7; formic acid, 64-18-6; glyoxylic acid, 298-12-4; mesoxalic acid, 473-90-5.

(9) Dolnik, M.; Marek, M. *J. Phys. Chem.* **1988**, *92*, 2452.

Study of the Thermal Dissociation of N_2O and CO_2 Using $O(^3P)$ Atomic Resonance Absorption Spectroscopy

Nobuyuki Fujii,* Shin-ichi Sagawai, Takashi Sato, Yoshio Nosaka, and Hajime Miyama

Department of Chemistry, Nagaoka University of Technology, Kamitomioka, Nagaoka 940-21, Japan
(Received: November 2, 1988; In Final Form: February 15, 1989)

The thermal dissociation of N_2O and CO_2 highly diluted in Ar was investigated in shock waves by measurement of $O(^3P)$ atomic resonance absorption. Observed formation rates of oxygen atoms behind the incident shock wave were compared with those obtained by computer simulation. The dissociation rate constants were determined to be as follows: For $N_2O + Ar \rightarrow N_2 + O + Ar$, $k_1 = 10^{15.0} \exp[(-251\ \text{kJ})/RT]$ ($cm^3\ mol^{-1}\ s^{-1}$). For $CO_2 + Ar \rightarrow CO + O + Ar$, $k_2 = 10^{13.4} \exp[(-364\ \text{kJ})/RT]$ ($cm^3\ mol^{-1}\ s^{-1}$).

Introduction

The dissociation of N_2O to N_2 and $O(^3P)$ is a typical example of spin-forbidden dissociation. It has been studied in detail with use of shock tubes.[1-3] The low preexponential factors found confirm that the reaction occurs via a spin-forbidden reaction path. The reported activation energy is considerably higher than the thermochemical ΔH°_{298} value of 167 kJ mol^{-1} for the reaction $N_2O \rightarrow N_2 + O(^3P)$ but lower than the ΔH°_{298} value of 357 kJ mol^{-1} for the spin-allowed reaction $N_2O \rightarrow N_2 + O(^1D)$. Accordingly, the activation energy is considered to be the energy of the crossing of the two surfaces.[1,2]

(1) Troe, J.; Wagner, H. Gg. In *Physical Chemistry of Fast Reactions*; Levitt, B. P., Ed.; Plenum Press: London, 1973; Vol. 1, p 1.
(2) Baulch, D. L.; Drysdale, D. D.; Duxbury, J.; Grant, S. *Evaluated Kinetic Data for High Temperature Reactions*; Butterworth: London, 1976; Vol. 3.
(3) Hanson, R. K.; Salimian, S. In *Combustion Chemistry*; Gardiner, W. C., Jr., Ed.; Springer-Verlag: New York, 1984; p 361.

0022-3654/89/2093-5474$01.50/0 © 1989 American Chemical Society

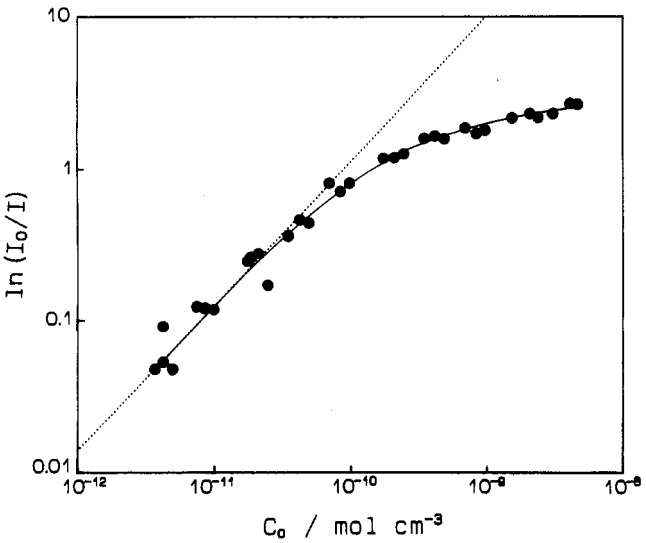

Figure 1. Calibration curve of O atom vacuum-UV absorption at 130 nm. Absorbance ln (I_0/I) is plotted against O atom concentration C_O. Dotted line shows the relation of Beer's law.

Another spin-forbidden dissociation of CO_2 has also been studied at high temperature by many researchers. The agreement among the reported rate constants is only fair, within a factor of about 10.[1,4,5] The reported activation energy values are much smaller than the ΔH°_{298} value of 532 kJ mol^{-1} for $CO_2 \rightarrow CO + O(^3P)$. This result is unusual, and two-step mechanisms of the dissociation kinetics have been proposed.[1,4] However, they have some inconsistency with experimental results, and it seems that the problem remains unsolved. It is worthwhile to measure the rate constant more accurately, especially by monitoring the $O(^3P)$ concentration, in order to reevaluate whether these low activation energies are correct.

Previously, the authors investigated the reaction kinetics of the N_2O–Ar system by measuring N_2O IR emission behind shock waves. The rate constant of N_2O unimolecular dissociation was reported.[6] Also, the authors studied the reaction kinetics of the CO–N_2O–Ar system by measuring CO and CO_2 IR emission behind shock waves, reported the termolecular recombination rate constant of $CO + O + Ar \rightarrow CO_2 + Ar$, and clarified the reaction mechanism.[7,8] The main objective of the present work is to examine the rate constant of the dissociation of CO_2 in a very dilute and pure system by measuring the concentration of the $O(^3P)$ atom spectroscopically in incident shock waves. The decomposition of N_2O was studied in incident shock waves first. Simulation of the reaction was carried out, and the results were compared with the experiments. After the comparison confirmed the accuracy of this experimental technique, the dissociation of CO_2 was studied.

Experimental Section

The experiments were carried out in a 46-mm-i.d. stainless steel shock tube. Its driven section is 3.6 m long and bakable up to about 100 °C. A pair of MgF_2 observation windows and a piezoelectric pressure gauge were located 3.1 m downstream from the diaphragm. The shock tube had a leak rate less than 5×10^{-4} Torr min^{-1} and was evacuated to less than 2×10^{-5} Torr before each run. The shock tube and related instruction have been described in more detail elsewhere.[6]

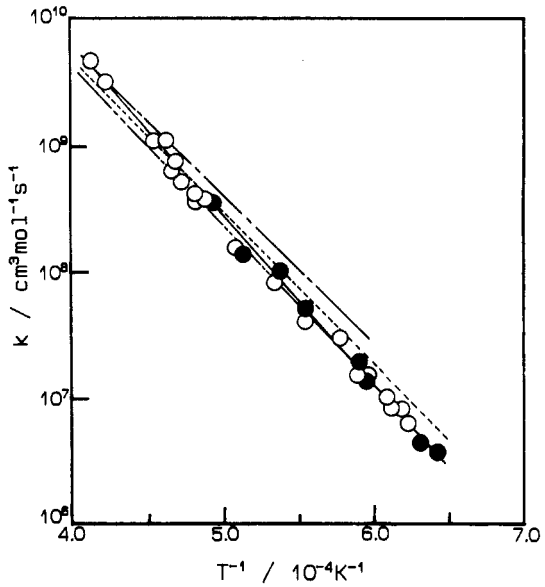

Figure 2. Arrhenius plots of rate constant k_1 for $N_2O + Ar \rightarrow N_2 + O + Ar$: ○, this work; ●, those obtained by N_2O IR emission;[6] —, this work; - - -, Baulch et al.;[1] - -, Hanson et al.;[3] - - -, Sulzmann et al.[12]

Atomic resonance absorption at 130 nm was used to monitor the time history of the oxygen atom concentration. The source of resonance radiation was a microwave discharge lamp in a flow of 10% O_2 diluted with He at a pressure of about 5 Torr. The transmitted light was measured by using a vacuum-UV monochromator (Ritsu MCV-20) and a solar-blind photomultiplier. The absorption signal and a pressure profile were displayed on a digital storage oscilloscope. Calibration of oxygen atom absorption was carried out with shock-heated N_2O–Ar mixtures. At temperatures above 2500 K, partial equilibrium in the dissociation of N_2O was achieved within the observation time. The calibration curve obtained in 1–1000 ppm N_2O in argon is shown in Figure 1. Here, no temperature dependence was observed in the temperature range 2500–3500 K. The signal to noise ratio was about 10; accordingly, the detection limit of O atom absorption was about 5×10^{-12} mol cm^{-3}. Also, the background absorption of N_2O and CO_2 was measured. The values of the absorption cross sections were almost constant in the observed temperature range.

$$\sigma(N_2O) = 8.8 \times 10^{-17}\ \text{cm}^2 \qquad 800\text{–}1300\ \text{K}$$

$$\sigma(CO_2) = 2.4 \times 10^{-18}\ \text{cm}^2 \qquad 1500\text{–}2000\ \text{K}$$

These values are almost the same as values reported previously.[9,10] Experiments were carried out on a mixture of N_2O (100 ppm) with Ar and on mixtures of CO_2 (500 and 1000 ppm) with argon. The gases used in the experiments were obtained from commercial suppliers. The stated purities of the gases were as follows: N_2O, 98% ($O_2 \leq 1.4\%$, $N_2 \leq 0.6\%$, $H_2O \leq 600$ ppm); CO_2, 99.99%; Ar, 99.998%. N_2O was purified by trap-to-trap distillation using dry ice and liquid N_2; the other gases were used without further purification.

Results and Discussion

(1) Dissociation of N_2. The dissociation of N_2O diluted in Ar was investigated behind incident shock waves in the temperature range 1600–2500 K at a total pressure of about 1 atm. The absorption profile obtained was compared with that derived from the calculated change of O atom concentration by using the calibration curve. The heat of reaction and the correction for the nonideality of shocked flow caused by the boundary layer behind the incident shock front[11] were taken into account. It was found by preliminary calculation that the formation of O atom was only

(4) Baulch, D. L.; Drysdale, D. D.; Horne, D. G.; Lloyd, A. C. *Evaluated Kinetic Data for High Temperature Reactions*, Butterworth: London, 1973; Vol. 2.
(5) Warnatz, J. In *Combustion Chemistry*; Gardiner, W. C., Jr., Ed.; Springer-Verlag: New York, 1984; p 197.
(6) Fujii, N.; Uchida, S.; Sato, H.; Fujimoto, S.; Miyama, H. *Bull. Chem. Soc. Jpn.* **1986**, *59*, 3431.
(7) Fujii, N.; Kakuda, T.; Sugiyama, T.; Miyama, H. *Chem. Phys. Lett.* **1985**, *122*, 489.
(8) Fujii, N.; Kakuda, T.; Takeishi, N.; Miyama, H. *J. Phys. Chem.* **1987**, *91*, 2144.
(9) Saito, K.; Bradley, J. N., unpublished data.
(10) Frank, P.; Just, Th. *Ber. Bunsen-Ges. Phys. Chem.* **1985**, *89*, 181.
(11) Fujii, N.; Koshi, M.; Ando, H.; Asaba, T. *Int. J. Chem. Kinet.* **1979**, *11*, 285.

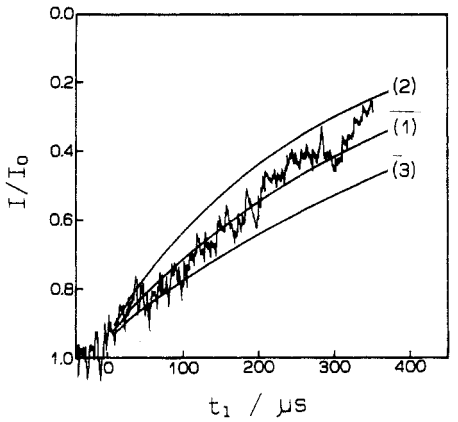

Figure 3. Example of the comparison of the experimentally obtained oxygen atom vacuum-UV absorption profile with simulated ones for 0.1% CO_2 in Ar (lines). T_2 = 2744 K, P_2 = 1.09 atm. Lines: (1) profile calculated with $k_2 = 2.49 \times 10^6$ ($=k_{2,s}$), (2) $k_2 = 1.5 \times k_{2,s}$, and (3) $k_2 = k_{2,s}/1.5$.

due to unimolecular dissociation of N_2O and was not affected by the subsequent reactions $N_2O + O \rightarrow NO + NO$ and $N_2O + O \rightarrow N_2 + O_2$ under the experimental conditions used. Accordingly, the rate constant k_1 of the dissociation

$$N_2O + Ar \rightarrow O + N_2 + Ar \qquad (1)$$

was obtained from the initial slope of O atom formation. The plot of k_1 (Figure 2) has the Arrhenius expression

$$k_1 = 10^{15.0\pm0.1} \exp[(-253.0 \pm 5\ \text{kJ})/RT]\ (\text{cm}^3\ \text{mol}^{-1}\ \text{s}^{-1}) \qquad 1600\text{–}2500\ \text{K}$$

In Figure 2, the rate constants obtained are compared with earlier values measured with N_2O infrared emission by the authors[6] and with those recommended by Baulch et al.,[2] Hanson et al.,[3] and Sultzmann et al.[12] Agreement among the values obtained in the present experiment and the previously reported values is good. From the comparison, it was confirmed that the present shock tube technique coupled with the atomic resonance absorption spectrometry has good accuracy.

(2) Dissociation of CO_2. The experiments were performed in the temperature range 2300–3400 K at pressures from 0.95 to 1.20 atm. A typical profile of 130-nm vacuum-UV absorption in a mixture of CO_2 in Ar behind a reflected shock wave is shown in Figure 3. After the initial rise of absorption due to shock-heated CO_2, the absorption due to $O(^3P)$ atom formation increases almost linearly. The initial slope due to $O(^3P)$ formation was found to be nearly proportional to the initial CO_2 concentration. The slope data for the CO_2 = 0.05 and 0.1% mixtures at various temperature are shown in Figure 4, where they are normalized by dividing by the total gas concentration immediately after the incident shock front, $[M]_0$. The absorption profiles were compared with those obtained by a computer simulation, in which the concentrations of $O(^3P)$ atom produced via the dissociation of CO_2 were converted into the absorption profile by using the calibration curve shown in Figure 1. The effect of wall boundary layer growth[11] was considered. Comparisons were made in the initial stage of reaction, within about 200 μs, where the effect of the boundary layer behind the shock front is not large. Examples of the comparison are shown in Figure 3. It was also found by computer simulation that the subsequent reactions $CO_2 + O \rightarrow CO + O_2$ and $O + O + Ar \rightarrow O_2 + Ar$ do not affect the absorption profile. Accordingly, the second-order rate constant k_2 of the dissociation

$$CO_2 + Ar \rightarrow O + CO + Ar \qquad (2)$$

was obtained from the initial slope of the O atom formation. The rate constants derived are also listed with the experimental con-

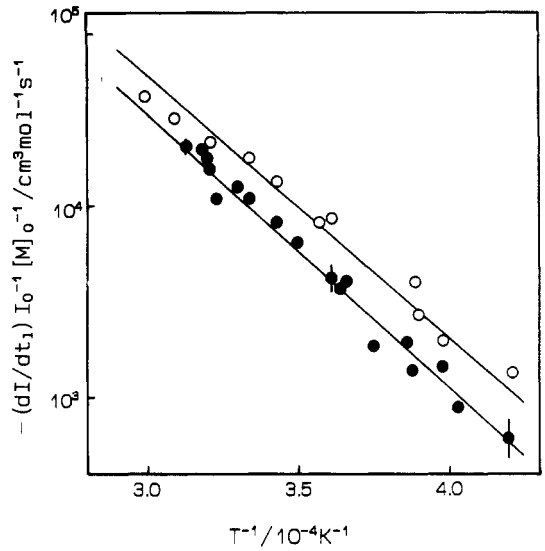

Figure 4. Temperature dependence of the initial growth rate of O atom vacuum-UV absorption: ○, CO_2, 0.1%; ●, CO_2, 0.05%.

TABLE I: Experimental Conditions and k_2 Values Obtained

run	CO_2, %	T_2, K	P_2, atm	ρ_2/ρ_1	k_2, cm^3 mol^{-1} s^{-1}
A-01	0.05	2389	1.120	3.540	2.2×10^5
A-02	0.05	2997	1.154	3.634	1.1×10^7
A-03	0.05	2919	1.215	3.624	7.5×10^6
A-04	0.05	2745	1.178	3.600	3.0×10^6
A-05	0.05	2732	1.085	3.598	3.5×10^6
A-06	0.05	2515	1.187	3.563	6.4×10^6
A-07	0.05	3129	1.109	3.649	2.2×10^7
A-08	0.05	2479	1.090	3.557	4.0×10^5
A-09	0.05	2588	1.021	3.575	9.4×10^5
A-10	0.05	2859	1.050	3.616	5.8×10^6
A-11	0.05	2575	0.975	3.573	1.0×10^6
A-12	0.05	2773	1.103	3.604	3.3×10^6
A-13	0.05	3112	1.153	3.647	1.6×10^7
A-14	0.05	2665	1.013	3.588	1.5×10^6
A-15	0.05	3096	1.196	3.645	1.2×10^7
A-16	0.05	3030	1.216	3.638	1.3×10^7
B-01	0.10	2513	1.108	3.566	3.6×10^5
B-02	0.10	2562	1.051	3.575	7.7×10^5
B-03	0.10	2799	1.072	3.611	2.9×10^6
B-04	0.10	2918	1.028	3.627	6.7×10^6
B-05	0.10	3145	0.964	3.655	1.7×10^7
B-06	0.10	3111	0.953	3.651	1.8×10^7
B-07	0.10	3128	0.958	3.653	1.6×10^7
B-08	0.10	3344	1.032	3.676	4.9×10^7
B-09	0.10	3233	0.993	3.664	3.1×10^7
B-10	0.10	3111	1.003	3.651	1.2×10^7
B-11	0.10	2996	1.010	3.637	1.0×10^7
B-12	0.10	2772	0.971	3.607	3.7×10^6
B-13	0.10	2574	0.976	3.577	1.2×10^6
B-14	0.10	2744	1.091	3.603	2.5×10^6
B-15	0.10	2377	0.966	3.541	2.4×10^5

ditions in Table I. The Arrhenius plot of k_2 is shown in Figure 5. The Arrhenius expression by a least-squares fit to the data was obtained:

$$k_2 = 10^{13.4\pm0.1} \exp[(-364.0 \pm 5\ \text{kJ})/RT]\ (\text{cm}^3\ \text{mol}^{-1}\ \text{s}^{-1}) \qquad 2300\text{–}3400\ \text{K}$$

The rate constants obtained are compared with the values reported for the CO_2–Ar system by Steinberg,[13] Olshewski et al.,[14] Dean,[15] and Wagner et al.[16] in Figure 6. Almost all rate data reported

(12) Sulzmann, K. G. P.; Kline, J. M.; Penner, S. S. *Twelfth Symposium (International) on Combustion*; The Combustion Institute: Pittsburgh, 1969; p 465.

(13) Steinberg, M. *NASA Contract. Rep.* 1965, *NASA CR-166*.

(14) Olschewski, H. A.; Troe, J. A.; Wagner, H. Gg. *Eleventh Symposium (International) on Combustion*; The Combustion Institute: Pittsburgh, 1967; p 155.

(15) Dean, A. M. *J. Chem. Phys.* **1973**, *58*, 5202.

(16) Wagner, H. Gg.; Zabel, F. *Ber. Bunsen-Ges. Phys. Chem.* **1974**, *78*, 705.

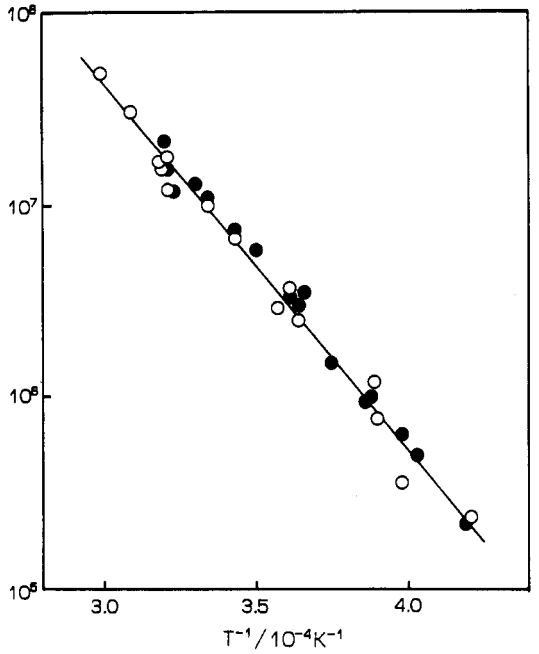

Figure 5. Arrhenius plot of k_2 for $CO_2 + Ar \rightarrow CO + O + Ar$: ○, CO_2, 0.1%; ●, CO_2, 0.05%.

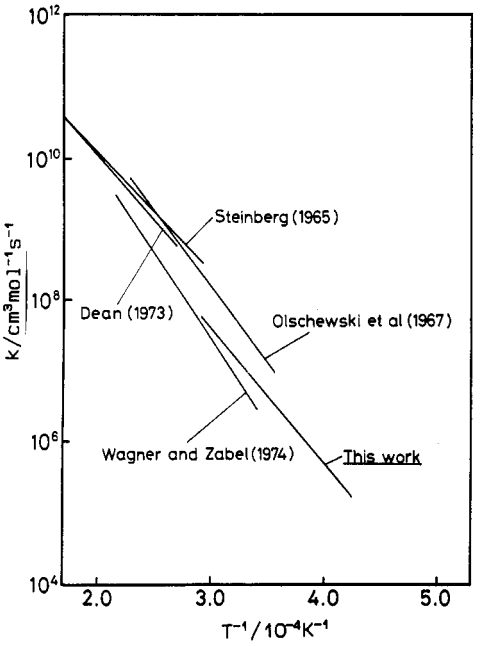

Figure 6. Comparison of Arrhenius plot of k_2 with those by other researchers.

previously were obtained by the direct or indirect measurement of the CO_2 concentration change, and no measurement of $O(^3P)$ has been reported. Also, in the present work, the rate constants were measured at lower temperatures than in previous work, because of the high sensitivity of the atomic resonant absorption method. The activation energy obtained in the present work is somewhat lower than values reported previously, but the agreement between the rate constants obtained in the present experiment and the previously reported values is good. The rate constants are also compared with the values[17-20] obtained from the rate constants

(17) Brabbs, T. A.; Belles, F. E. *Eleventh Symposium (International) on Combustion*; The Combustion Institute: Pittsburgh, 1967; p 125.
(18) Lin, M. C.; Bauer, S. H. *J. Chem. Phys.* **1969**, *50*, 3377.
(19) Brown, W. G.; White, D. R.; Smookler, G. R. *Twelfth Symposium (International) on Combustion*; The Combustion Institute: Pittsburgh, 1969; p 557.
(20) Wagner, H. Gg. Proceedings of the Eighth International Shock Tube Symposium, 1971; No. 4.

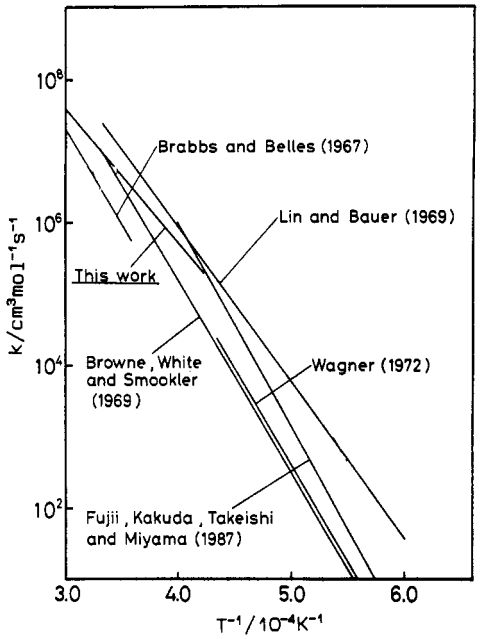

Figure 7. Comparison of Arrhenius plot of k_2 obtained with those obtained from the rate of the reverse reaction $CO + O + Ar \rightarrow CO_2 + Ar$.

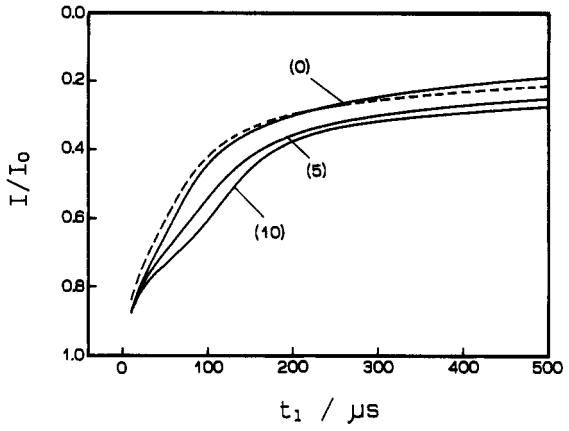

Figure 8. Effect of C_2H_6 contamination on computed oxygen atom profiles in an incident shock wave in $CO_2/Ar = 0.1/99.9$ with $P_1 = 30$ Torr and $T_5 = 2500$ K. Line numbers 0, 5, and 10 mean that the amount of $[C_2H_6]$ in test gas is 0, 5, and 10 ppm, respectively. Dotted line shows the calculated value from k_1 multiplied by 1.5 in the mixture containing 5 ppm C_2H_6.

of the recombination reaction $CO + O + Ar \rightarrow CO_2 + Ar$, including those measured with CO_2 infrared emission by the authors[8] in Figure 7. From these two figures, the rate constant of the CO_2 dissociation seems to be expressed by one equation from low to high temperature, but the apparent activation energy appears to decrease with increasing temperature.

It has been discussed that uncertainties due to influences of impurities such as H_2O and hydrocarbons have affected the reported activation energies for CO_2 dissociation. In the present work, the effect of contaminants upon oxygen atom formation was investigated in the following manner. Simulations using a mechanism[8] for the oxidation of small hydrocarbons were carried out for test gas mixtures that were assumed to contain C_2H_6 at 1, 5, and 10 ppm as contaminants in addition to the CO_2 component of the test gas used in the present experiments. An example of the calculated O atom absorption profiles is shown in Figure 8. It can be seen that, in spite of an increase in CO_2 dissociation rate, the rate of O atom formation is retarded by these assumed contaminant concentrations, but the effect is not so large. For example, the rate constant of the dissociation reaction increases by about 1.5 if the amount of the assumed contaminant C_2H_6 is 5 ppm. Also, the calculated profile of O atom formation does not have a linear increase with time in the initial stage of the

reaction as shown in Figure 8, when the amount of the assumed impurity C_2H_6 is larger than 10 ppm. This was not observed in the experiment. Accordingly, the effect of the impurity on the rate constant of the dissociation seems to be less than a factor of 1.5 and is then not so serious in the present work.

As described above, the activation energy for the N_2O dissociation was well explained by a crossing of two potential surfaces. However, from the fact that the activation energy is remarkably lower than the bond dissociation energy, the mechanism for CO_2 dissociation must be more complicated. The mechanism for this spin-forbidden dissociation proposed by Brabbs et al.[17] is

$$CO_2(^1\Sigma) + M \rightarrow CO_2(^3\Pi) + M$$

$$CO_2(^3\Pi) \rightarrow CO(^1\Sigma) + O(^3P)$$

while that proposed by Fishburne et al.[21] is

$$CO_2(^1\Sigma) + M \rightarrow CO_2^* + M$$

$$CO_2^* \rightarrow CO(^1\Sigma) + O(^3P)$$

where CO_2^* is $CO_2(^3B_2)$ or $CO_2(^1B_2)$. In both mechanisms, the first excitation step was assumed to be slow compared with the dissociation step. Also, in both mechanisms, the crossing point between the surfaces of ground state and the excited states were assumed to be far below the dissociation limit to $CO(^1\Sigma) + O(^3P)$. However, if the crossing occurs at lower energy than the bond energy, additional energy is required for dissociation. Therefore, both mechanisms are not satisfactory to explain the low activation energy.

On the other hand, the RRK unimolecular rate theory expression $k = A(D/RT)^{s-1.5} \exp(-D/RT)$ has been applied to the rate constants of this reaction,[21,22] where D represents the bond dissociation energy and s is the number of effective freedoms of vibration. When the theory was applied to the present data, A and s were found to be 5.2×10^6 cm^3 mol^{-1} s^{-1} and 7.2, respectively. In most cases, including the present study, except for a few works,[23] the values of s were higher than 4, which is the number of degrees of vibrational freedom of CO_2. Accordingly, the application of RRK theory to the CO_2 dissociation is not justified.

Therefore, some other mechanism must be proposed. For this purpose, the potential energy surfaces of CO_2 must be determined by more refined spectroscopic experiments.

In summary, measurements of N_2O dissociation rates were performed at first, and the rate constants agreed well with the values reported previously. Then, measurements of CO_2 dissociation rates were carried out by monitoring $O(^3P)$ absorption in highly dilute CO_2–Ar mixtures at lower temperatures than previous work (2300–3400 K). The activation energy of the rate constant was somewhat lower than previously reported values, while the rate constant values are in agreement with previous data. Accordingly, it was confirmed that the rate data obtained previously were those for the spin-forbidden reaction. However, a more detailed reaction scheme cannot be proposed in the present work, because of lack of detailed information about the CO_2 potential surfaces.

Acknowledgment. We thank Dr. K. Saito of Hiroshima University for discussions and T. Hashimoto and T. Arii for their help in preliminary experiments. This work was partially supported by a Secom Foundation Research Grant, for which we express our thanks.

Registry No. N_2O, 10024-97-2; CO_2, 124-38-9.

(21) Fishburne, E. S.; Bilwakesh, K. R.; Edse, R. *J. Chem. Phys.* **1966**, *45*, 160.

(22) Kuratani, K.; Tsuchiya, S. *Chemical Physics of Shock Waves*; Syouka-bou: Tokyo, 1968; p 219.

(23) Kiefer, J. H. *J. Chem. Phys.* **1974**, *61*, 244.

Photochemistry of Nitrosyl Porphyrins in the Temperature Range 180–300 K and the Effects of Pyridine on Photodenitrosylation of Nitrosyliron Tetraphenylporphyrin

Mikio Hoshino* and Mieko Kogure

The Institute of Physical and Chemical Research, Wako, Saitama, 351-01, Japan
(Received: November 8, 1988)

Nitrosylmetal tetraphenylporphyrin (NOMTPP, M = Fe, Co, and Mn) in benzene solutions undergoes facile photodenitrosylation to give NO and metal(II) tetraphenylporphyrin, M^{II}TPP. The photodenitrosylation yields of NOFeTPP and NOCoTPP are respectively determined as 0.50 ± 0.05 and 1.0 ± 0.05 at both excitation wavelengths 355 and 532 nm. The yield, Φ, in toluene is expressed as a function of temperature: $\Phi = (1 + 1.56 \times 10^{-2} \exp(2400/RT))^{-1}$ for NOFeTPP and $\Phi = (1 + 1.02 \times 10^{-6} \exp(5200/RT))^{-1}$ for NOCoTPP. Contrary to NOFeTPP and NOCoTPP, the photodenitrosylation yields, Φ, of NOMnTPP are independent of temperature in the range 300–180 K and exhibit excitation wavelength dependence: $\Phi = 0.78 \pm 0.05$ at 355 nm and $\Phi = 0.62 \pm 0.05$ at 532 nm. The effects of the central metal on photodenitrosylation are described. The laser photolysis of NOFeTPP in the presence of low concentration of pyridine revealed that the Fe^{II}TPP initially produced reacts with a pyridine molecule, Py, to form five-coordinate (Py)Fe^{II}TPP. The five-coordinate (Py)Fe^{II}TPP further reacts with Py to give six-coordinate $(Py)_2Fe^{II}$TPP, which recombines with NO to regenerate NOFeTPP. The kinetic study has demonstrated that the five-coordinate (Py)Fe^{II}TPP which is in equilibrium with $(Py)_2Fe^{II}$TPP is responsible for the recombination reaction of $(Py)_2Fe^{II}$TPP and NO.

Introduction

Hemoproteins which dominate storage and transportation of oxygen in life have been the subject of extensive studies by optical, ESR, and Mössbauer methods[1-4] as well as by X-ray crystal structure determinations.[2,3] These proteins are known to react readily with simple diatomic molecules, O_2, NO, and CO to give their adducts.[1,5,6] It has long been recognized that these adducts undergo dissociation of O_2, NO, or CO by photolysis.[7-16] For

(1) James, B. R. In *The Porphyrins*; Dolphin, D., Ed.; Academic Press: New York, 1978; Vol. V, Chapter 6.

(2) Antonini, E.; Brunori, M. In *Frontiers of Biology*; Neuberger, A., Tatum, E. L., Eds.; North-Holland: Amsterdam, 1971; Vol. 21.

(3) Antonini, E.; Brunori, A. *Annu. Rev. Biochem.* **1970**, *39*, 977–1042.

(4) Münck, E. In *The Porphyrins*; Dolphin, D., Ed.; Academic Press: New York, 1978; Vol. IV, Chapter 8.

(5) Chien, J. C. W. *J. Am. Chem. Soc.* **1969**, *91*, 2166–2168.

(6) Doetschmann, D. C.; Utterback, S. G. *J. Am. Chem. Soc.* **1981**, *103*, 2847–2852.

0022-3654/89/2093-5478$01.50/0 © 1989 American Chemical Society